


Article

# Cellulose Nanocrystals from Fibers of Macauba (*Acrocomia Aculeata*) and Gravata (*Bromelia Balansae*) from Brazilian Pantanal

Ana Carolina Corrêa <sup>1,\*</sup> , Vitor Brait Carmona <sup>1,2</sup>, José Alexandre Simão <sup>1,2</sup>, Fabio Galvani <sup>3</sup>, José Manoel Marconcini <sup>1</sup> and Luiz Henrique Capparelli Mattoso <sup>1</sup>

<sup>1</sup> Nanotechnology National Laboratory for Agriculture (LNNA), Embrapa Instrumentation, P.O. Box 741, 13560-970 São Carlos, SP, Brazil; brait\_carmona@hotmail.com (V.B.C.); alexandre\_simao1@hotmail.com (J.A.S.); jose.marconcini@embrapa.br (J.M.M.); luiz.mattoso@embrapa.br (L.H.C.M.)

<sup>2</sup> Graduate Program in Materials Science and Engineering (PPGCEM), Federal University of São Carlos (UFSCar), Rod. Washington Luiz, Km 235, 13565-905 São Carlos, SP, Brazil

<sup>3</sup> Embrapa Pantanal, P.O. Box 109, 79320-900 Corumbá, MS, Brazil; fabio.galvani@embrapa.br

\* Correspondence: carol\_correa@hotmail.com

Received: 21 September 2019; Accepted: 21 October 2019; Published: 1 November 2019



**Abstract:** Cellulose nanocrystals (CNC) were obtained from macauba and gravata fibers. Macauba (or Bocaiuva) is a palm tree found throughout most of Brazil and Gravata is an abundant kind of bromelia with 1–2m long leaves, found in Brazilian Pantanal and Cerrado. The raw fibers of both fibers were mercerized with NaOH solutions and bleached; they were then submitted to acid hydrolysis using H<sub>2</sub>SO<sub>4</sub> at 45 °C, varying the hydrolysis time from 15 up to 75 min. The fibers were analyzed by X-ray diffraction (XRD), FTIR Spectroscopy, scanning electron microscopy (SEM) and thermal stability by thermogravimetric analysis (TG). XRD patterns did not present changes in the crystal structure of cellulose after mercerization, but it was observed a decrease of hemicellulose and lignin contents, and consequently an increase of cellulose content with the increase of NaOH solution concentration in the mercerization. After acid hydrolysis, the cellulose nanocrystals (CNC) were also analyzed by transmission electron microscopy (TEM) which showed an acicular or rod-like aspect and nanometric dimensions of CNC from both fibers, but the higher values of aspect ratio (L/D) were found on CNC obtained from gravata after 45 min of acid hydrolysis. The mercerization and subsequent bleaching of fibers influenced the crystallinity index and thermal stability of the resulting CNC, but their properties are mainly influenced by the hydrolysis time, i. e., there is an increase in crystallinity and thermal stability up to 45 min of hydrolysis, after this time, both properties decrease, probably due to the cellulose degradation by the sulfuric acid.

**Keywords:** cellulose nanocrystals; pantanal fibers; gravata; macauba; characterization

## 1. Introduction

Cellulose is a natural semi-crystalline polymer consisting of glucose repeating units bounded by β-1,4-glycosidic bonds; it can be produced and obtained from plants, bacteria and even some animals [1,2]. Cellulose nanocrystals (CNC) are rod-like and highly crystalline materials with diameters in the range of 5–70 nm and lengths from 100nm up to a few microns. CNC can be obtained by the acid hydrolysis of high content semi-crystalline cellulose materials, such as vegetable fibers [3].

CNC are produced by the crystalline fraction exposure of cellulose fibers to strong acid hydrolysis. The chemical process starts with the removal of superficial polysaccharides followed by cleavage and destruction of amorphous fractions of cellulose. To end the reaction, the acid solution must be

diluted and separated from the CNC by means of centrifugation and dialysis. Then, CNC should be redispersed by ultrasound producing stable suspensions. Both structure, properties and suspension behavior of CNC depends on concentrations and type of used acid, hydrolysis temperature and time and of intensity of ultrasound energy [3–5].

CNC can present different morphologies, dimensions and crystallinity depending on material source and the fiber pre-treatment, i.e., bleaching, mercerizing or using raw fibers, as well the time, temperature, acid type and concentration on acid hydrolysis [6].

CNC stable suspensions can be produced using concentrated solutions of H<sub>2</sub>SO<sub>4</sub> and also HCl followed by sonication, and the first report of such a process was made by Ranby in 1951 [7]. Since then, CNC has been obtained via acid hydrolysis from various materials such as tunicates [8], microbial cellulose [9], Kraft pulp [10], microcrystalline cellulose [4] and vegetable fibers such as cotton [11,12], sugar-cane bagasse [13], sisal [14,15] and curaua [16].

The type of acid strongly affects superficial properties of CNC. CNC obtained from HCl hydrolysis tend to form aggregates [9,17], whereas those obtained from H<sub>2</sub>SO<sub>4</sub> hydrolysis are stable and better dispersed due to the ester-sulphate electrostatic repulsion present on the crystal surfaces [18]. On the other hand, CNC morphology mainly depends on the cellulose source: CNC from tunicates and algae can have up to a few tens of microns in length, while vegetable fibers produce crystals with length in the order of hundreds of nanometers [3,8,18–20]. The type of acid plays important role on thermal stability of CNC as well. Better dispersed and surface charged CNC, obtained by H<sub>2</sub>SO<sub>4</sub> hydrolysis, can be up to 95 °C less thermally stable than those obtained by HCl hydrolysis (~200 °C vs. 295 °C, respectively), while CNC obtained by an acid mixture present intermediate properties [16,21].

The development of CNC-reinforced nanocomposites still require study and advance because of CNC low thermal stability compared to processing temperature of engineering polymers, as well their hydrophobic character and inherent difficulty of dispersion in nonpolar matrices. However, CNC has already been used as reinforcement polymer matrix based on polysaccharides or proteins, resulting in increased mechanical strength and barrier properties without compromising their biodegradability [22, 23].

Macauba (*Acrocomia aculeata*) and gravata (*Bromelia balansae*) present good properties and high content of cellulose [24,25], showing potential to be used as a source to obtain CNC. Macauba is an abundant palm tree found throughout most of Brazil, their leaves and nuts can be used as human and animal nutrition and for oil extraction, and their trunk can be used in civil construction. Gravata is an abundant kind of bromelia with 1–2m long leaves found in Pantanal and Brazilian Cerrado, their leaves are used to obtain natural fibers for handicrafts and ropes and their fruits (pulp and nuts) are appreciated by humans and animals [26]. Embrapa Pantanal manages a project with the Antonia Maria Coelho Community that aims to characterize the productive system of extracted products from macauba, like using its pulp and flour on vitamins, ice creams and breads, and its oil on biodiesel production. All these activities contribute to generate wealth for local communities and helps to promote sustainable development by encouraging projects whose uses raw material from renewable sources, adding values to these products. Images of gravata and macauba are shown in Figure 1.

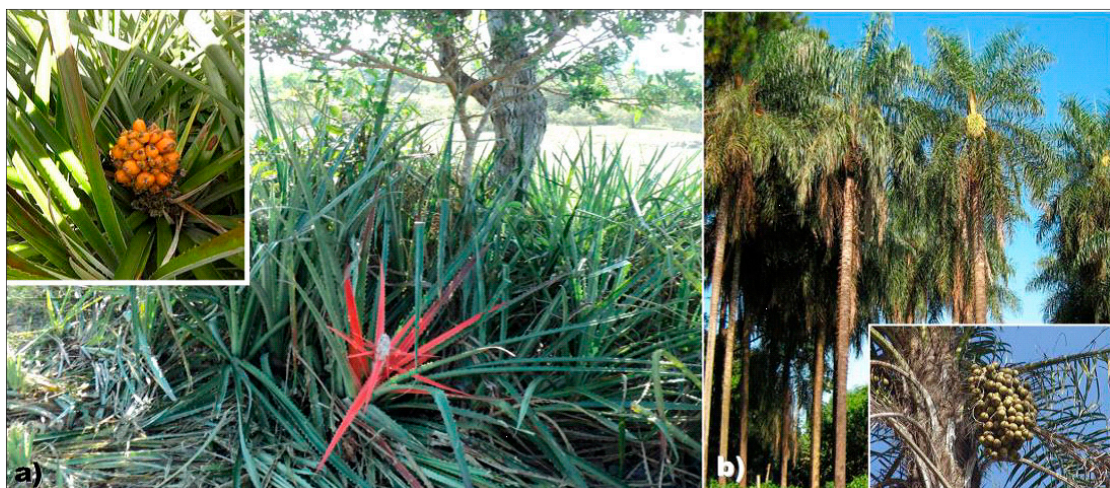


**Figure 1.** Images of (a) gravata and (b) macauba, with their respective fruits in detail.

Thus, this is an exploratory study, proposing the use of byproducts (rachis, leaves and fruit pulp) of macauba and from gravata fibers, to obtain a cellulose rich material with potential to obtain cellulose nanocrystals (CNC), adding value to these materials and generating income for the local population. In this way, the aim of this study is the extraction and characterization of CNC from macauba and gravata. It will also be investigated the influence of different pre-treatment on raw fibers, using different concentrations of sodium hydroxide and peroxide solutions, and the influence of acid hydrolysis time on final properties of obtained CNC, such as thermal stability, crystallinity and morphology.

## 2. Experimental

### 2.1. Material and Methods

#### 2.1.1. Alkali Treatment of Gravata and Macauba Fibers

The CNCs from gravata and macauba was obtained from the fibers previously submitted to mercerization and/or bleaching, in order to achieve higher cellulose content and greater exposure of the cellulosic fibers. Gravata and Macauba raw fibers were gently supplied by Embrapa Pantanal (Corumbá, Brazil). The mercerization was carried out in sodium hydroxide (NaOH) solutions, and in order to evaluate the influence of the NaOH concentration on the alkaline solution for mercerization, 1%, 5% and 10% (*m/v*) of NaOH was applied. 20.0 g of fiber were placed in 300 mL of alkali solution at 60 °C, and submitted to mechanical stirring at 3000 rpm for 60 min.

It was also evaluated the influence of alkaline and peroxide concentration on the removal of non-cellulosic components from the fiber. Hydrogen peroxide was added to the alkaline solution in the amount that the final solution had the concentration determined in Table 1. Around 20 g of fibers were added to the hydrogen peroxide alkali solution at 60 °C and they were mechanical stirred for 60 min. The conditions of mixing, temperature and reaction time were kept constant to mercerization and bleaching processes. Furthermore, a bleaching treatment of each fiber was selected and repeated in the already bleached fiber under the same conditions of stirring, temperature and reaction time.

**Table 1.** Gravata and macauba fiber samples under different mercerization and bleaching treatments.

Sample	Pretreatment	[NaOH] (m/v)	[H <sub>2</sub> O <sub>2</sub> ] (v/v)
gra	None	-	-
gra_m1	Mercerization	1%	-
gra_m2	Mercerization	5%	-
gra_m3	Mercerization	10%	-
gra_b1	Bleaching	5%	1%
gra_b2	Bleaching	5%	5%
gra_b3	Bleaching	5%	10%
gra_b2_2X	Bleaching (2X)	5%	5%
mac	None	-	-
mac_m1	Mercerization	1%	-
mac_m2	Mercerization	5%	-
mac_m3	Mercerization	10%	-
mac_b1	Bleaching	10%	1%
mac_b2	Bleaching	10%	5%
mac_b3	Bleaching	10%	10%
mac_b3_2X	Bleaching (2X)	10%	10%

All samples were filtered through a filter paper, washed until neutralization and dried in an air circulation oven at 60 °C for 24 h. Table 1 shows the encoding of the gravata and macauba fibers as a function of pretreatment.

#### 2.1.2. CNCs from Bleached Fibers Obtained by Acid Hydrolysis

The hydrolysis process was carried out based on previous studies, where conditions for other vegetable fibers such as cotton [12,21], curaua [16], sisal [14], eucalyptus [10], sugarcane bagasse [13], oil palm fibers [27], among others, were already established. From the bleached fibers, the acid hydrolysis was carried out adding 5 g of bleached fibers in 100 mL of 60% w/w H<sub>2</sub>SO<sub>4</sub> solution at 45 °C under vigorous stirring for different reaction time: 15, 30, 45, 60 and 75 min. The resulting suspensions were centrifuged twice for 10 min at 10,000 rpm, the supernatant was discarded, the sediment was redispersed in distilled water and dialyzed in water until neutral pH. The suspension was sonicated for 5 min, frozen and stored. Dry CNCs were obtained by lyophilization process.

Table 2 presents the coding of the CNC samples, obtained from macauba and gravata from the once or twice bleached fibers and after different hydrolysis time.

**Table 2.** CNC samples obtained from gravata and macauba, under different times of acid hydrolysis at 45 °C and from the once or twice bleached fibers.

Sample	Fiber	Hydrolysis Time (min)	Sample	Fiber	Hydrolysis Time (min)
CNCg_1_15	gra_b2	15	CNCm_1_15	mac_b3	15
CNCg_1_30	gra_b2	30	CNCm_1_30	mac_b3	30
CNCg_1_45	gra_b2	45	CNCm_1_45	mac_b3	45
CNCg_1_60	gra_b2	60	CNCm_1_60	mac_b3	60
CNCg_1_75	gra_b2	75	CNCm_1_75	mac_b3	75
CNCg_2_15	gra_b2_2X	15	CNCm_2_15	mac_b3_2X	15
CNCg_2_30	gra_b2_2X	30	CNCm_2_30	mac_b3_2X	30
CNCg_2_45	gra_b2_2X	45	CNCm_2_45	mac_b3_2X	45
CNCg_2_60	gra_b2_2X	60	CNCm_2_60	mac_b3_2X	60
CNCg_2_75	gra_b2_2X	75	CNCm_2_75	mac_b3_2X	75

## 2.2. Characterization

### 2.2.1. X-Ray Diffracton

The X-ray diffractograms of raw, pretreated fibers and CNCs were obtained on an X-ray diffractometer (Shimadzu, XRD-6000, Tokyo, Japan), operating at 30 kV / 30 mA, CuK $\alpha$  radiation ( $\lambda = 1.5406 \text{ \AA}$ ). The tests were conducted at room temperature and  $2\theta$  between 10 and  $30^\circ$  with a speed of  $1^\circ/\text{min}$ . The crystallinity indexes were calculated by deconvolution in peaks of the diffractograms, taking a Gaussian distribution function as crystalline and amorphous peaks. The OriginLab 8.0 software (OriginLab, Northampton, MA, USA) was used to estimate the crystallinity indexes ( $C_i$ ) based on the areas under the crystalline peaks and amorphous halo of cellulose after correction of the baseline, according to the method of Oh et al. [28]. Equation 1 was used to estimate  $C_i$ :

$$C_i (\%) = \left(1 - \frac{A_a}{A_t}\right) \times 100 \quad (1)$$

where,  $A_a$  is the area corresponding to the curve of the amorphous halo, and  $A_t$  is the sum of the areas of all crystalline and amorphous peaks.

### 2.2.2. Infrared Spectroscopy (FTIR)

FT-IR analyzes of raw, pretreated fibers and CNCs were performed on a Perkin Elmer Spectrum 1000 spectrometer (Perkin Elmer, Waltham, MA, USA). The spectra were obtained with 64 scans in the wavelength region of  $400$  to  $4000 \text{ cm}^{-1}$  and resolution of  $2 \text{ cm}^{-1}$ .

### 2.2.3. Termogravimetric Analysis (TGA)

The thermal stability of raw, pretreated fibers and CNCs were evaluated by thermogravimetry using TGA Q500 (TA Instrument, New Castle, DE, USA) equipment under synthetic air atmosphere at flow rate of  $60 \text{ mL/min}$ ; heating rate of  $10 \text{ }^\circ\text{C/min}$  and temperature range from  $25$  to  $600 \text{ }^\circ\text{C}$ . The onset temperature ( $T_{\text{onset}}$ ) was determined through the TG curve, as the intersection of the extrapolation line from the beginning of the thermal event with the tangent to the curve at the temperature of the maximum thermal degradation rate (obtained by the DTG curve) of the material.

### 2.2.4. Scanning electron microscopy (SEM)

SEM micrographs of the outer surface of the in natura and pretreated fibers were obtained on a JEOL scanning electron microscope (JSM-6510 series, Jeol Ltd., Tokyo, Japan), operating at  $10\text{kV}$ , and all samples were coated with gold.

### 2.2.5. Transmission Electron Microscopy (TEM)

Diluted suspensions of CNCs in water were prepared which were dispersed using Branson's tip ultrasound (Branson Ultrasonics, Danbury, CT, USA), with a  $1\text{cm}$  tip, at  $50\%$  power for  $2 \text{ min}$ . One drop of this suspension was placed on copper grids ( $400$  mesh, Ted Pella - No. 01822, Pelco Inc., Fresno, CA, USA) and dried at room temperature. After  $24 \text{ h}$ , the samples were stained with  $1.5\%$  uranyl acetate solution, deposited on the grids. The analyzes were performed on a Tecnai<sup>TM</sup> G2 F20 equipment (FEI Company, Hillsboro, OR, USA). The mean diameter as well as the mean length of the CNCs were calculated using ImageJ software (Bethesda, MD, USA) using at least  $50$  measurements in each dimension.

## 3. Results and Discussion

As the objective is to obtain cellulose nanocrystals, pre-treatments of mercerization and bleaching of the gravata and macauba fibers were carried out in order to extract the highest amount of hemicelluloses and lignin. The bleaching of both fibers was only carried out after prior characterization

of the mercerized fibers, determining the concentration of NaOH and H<sub>2</sub>O<sub>2</sub> in the alkaline peroxide solution used for bleaching. Figure 2 shows the gravata and macauba fibers after the mercerization and bleaching treatments.

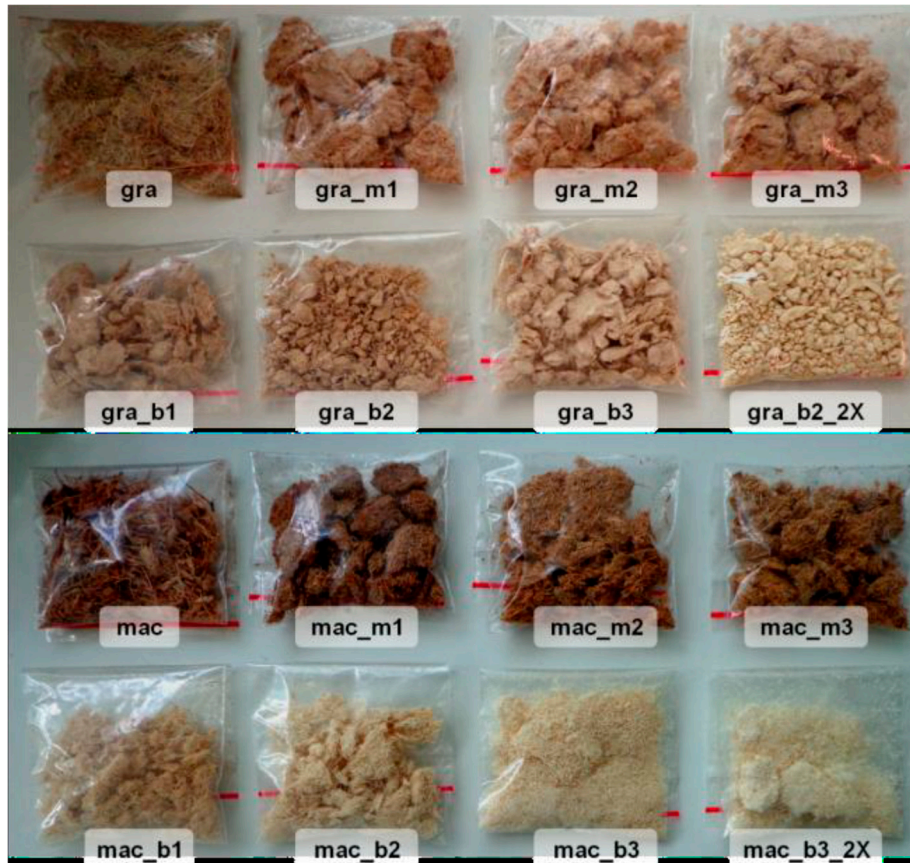


**Figure 2.** Images of raw fibers of gravata and macauba, and mercerized and bleached fibers, with their respective coding.

As can be observed in Figure 2, there was a gradual whitening of the gravata and macauba fibers as the NaOH concentration was increased for each mercerization treatment. The use of alkaline peroxide in bleaching treatments has led to even more intense whitening, especially for macauba fibers. This can be considered as an indication of the efficiency of the treatments in the removal of compounds such as hemicellulose and lignin from the gravata and macauba fibers.

Fibers Ci can be related to their cellulose contents [29]. Thus, its determination by XRD is a good parameter for the selection of the appropriate concentration of NaOH for the mercerization of the vegetal fibers, as well as the alkaline peroxide solutions in the bleaching treatments. The diffraction profiles of raw, mercerized and bleached fibers from gravata and macauba are shown in Figure 3.

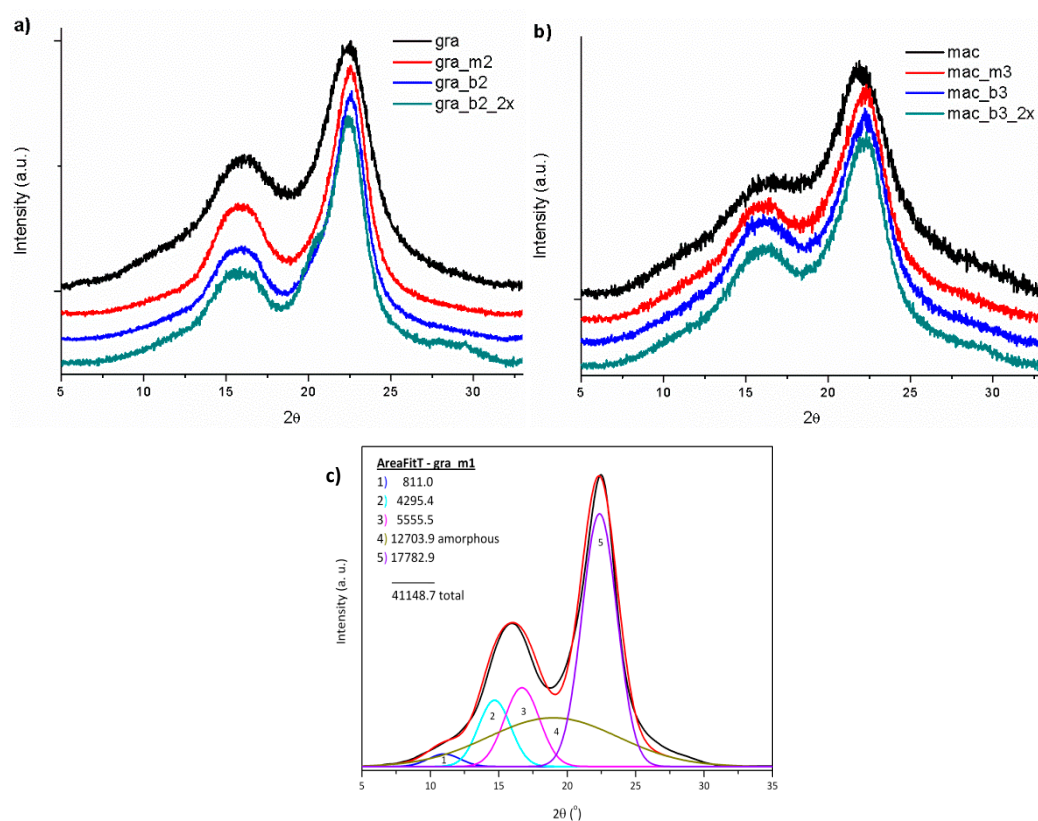


**Figure 3.** XRD profiles of raw, mercerized and bleached fibers from (a) gravata and (b) macauba, and (c) is an example of deconvoluted peaks for mercerized gravata fibers.

The XRD diffraction profiles of the fibers are similar to each other and show characteristic peaks of cellulose type I with diffraction peaks at  $2\theta = 15^\circ$ ,  $17^\circ$  and  $22.7^\circ$  [2]. The increase of NaOH concentration in solutions used for the mercerization and the increase of  $H_2O_2$  concentration in the subsequent bleaching treatments caused a narrowing and definition of the crystalline peaks, indicating a removal of amorphous materials, such as hemicellulose and lignin [29].

However, even increasing NaOH concentration to 10 wt% (in the solution used for mercerization), no polymorphic changes of cellulose type I (raw fibers) to cellulose type II (after the mercerization process) were observed, maintaining the crystalline structure of raw cellulose fibers [30].

It was observed an increase of the  $C_i$  with the increase of the NaOH concentration for the mercerization treatments and also with the increase of the  $H_2O_2$  concentration in the subsequent bleaching treatments, mainly for macauba samples, as presented in Table 3. And for both fibers, the repetition of the bleaching process provided an increase in the crystallinity of the fibers, which will be used to obtain the cellulose nanocrystals.

**Table 3.**  $T_{onset}$ , residues content and Ci of gravata and macauba raw, mercerized and bleached fibers.

Sample	$T_{onset}$ (°C)	Residues (%)	Ci (%)
gra	244	3.3	58
gra_m1	276	2.3	69
gra_m2	304	2.1	77
gra_m3	314	1.1	77
gra_b1	307	1.3	81
gra_b2	311	1.4	82
gra_b3	311	1.3	79
gra_b2_2X	302	1.3	86
mac	233	10.9	55
mac_m1	268	2.6	65
mac_m2	279	2.3	65
mac_m3	282	2.3	71
mac_b1	282	2.6	74
mac_b2	282	2.3	76
mac_b3	278	2.3	77
mac_b3_2X	284	1.1	83

For the gravata fibers, it can be observed that the increase of the NaOH concentration in the mercerization was efficient, resulting in an increase of the Ci using solution with up to 5% NaOH ( $m/v$ ), reaching Ci = 77% for gra\_m2. And maintaining the concentrations of 5% NaOH ( $m/v$ ) to prepare the alkaline peroxide solution for bleaching, it was observed an increase in Ci with the increase in the concentration of H<sub>2</sub>O<sub>2</sub> up to 5% ( $v/v$ ), reaching 82% of crystallinity for gra\_b2. Repeating this bleaching process, Ci = 86% was determined for gra\_b2\_2x. But even using a 10 wt% NaOH solution for mercerization and increasing the concentration of H<sub>2</sub>O<sub>2</sub> to 10 wt% in the alkaline peroxide for bleaching, it was not observed additional effects on the crystallinity of gravata fibers.

Regarding the macauba fibers, mercerization with a 10 wt% NaOH solution generated the highest Ci of 70.8% for mac\_m3. Thus, maintaining the concentration of 10 wt% NaOH for the alkaline peroxide solutions used for bleaching, and increasing the concentration to 10% H<sub>2</sub>O<sub>2</sub> ( $v/v$ ) in the alkaline peroxide solution, a Ci of 77% was calculated for mac\_b3; and after the repetition of this bleaching process, it was determined a Ci of 83% for mac\_b3\_2x. As macauba fibers present a higher non-cellulosic materials content than gravata fibers, like lignin and hemicellulose [24,25], it was expected to be necessary a more drastic treatment, in order to remove those substances.

In fact, what occurs is not an increase in the crystalline portion of the fibers but a removal of a greater part of the amorphous portion of the fibers, which can also be components of lower thermal stability. In this way, their removal result in an increase in thermal stability of the pre-treated fibers, as can be observed in Table 3. Thus, the mercerized fibers of gravata with 10wt% NaOH solution, presented an increase in thermal stability of up to 70 °C, reaching  $T_{onset}$  of around 314 °C. The subsequent bleaching treatments resulted in fibers with  $T_{onset}$  ranging from 302 to 311 °C.

Regarding the macauba fibers, the bleaching treatment resulted in an increase of up to 50°C in thermal stabilities ( $T_{onset}$  = 284 °C for mac\_b3\_2x). The  $T_{onset}$  of the remaining macauba fibers were determined in the range of 268 °C to 282 °C, much more thermally stable than fibers “in natura”, which shows the necessity of the pre-treatments of mercerization and/or bleaching of the vegetal fibers before the process of acid hydrolysis to obtain cellulose nanocrystals.

Figure 4 shows the TG and DTG curves of the gravata and macauba fibers and their thermal behavior.



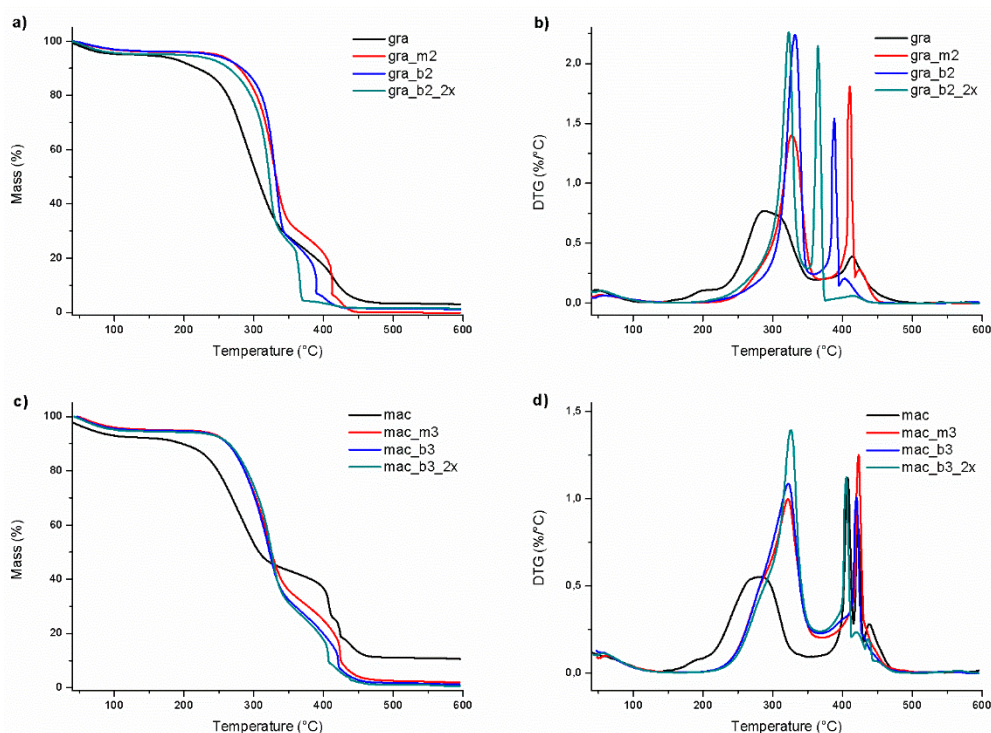


**Figure 4.** Thermograms (a) TG and (b) DTG curves of gravata raw, mercerized and bleached fibers, (c) TG and (d) DTG curves of macauba raw, mercerized and bleached fibers, in synthetic air atmosphere and heating rate of 10 °C/min.

In general, there is a first stage of mass loss occurring between room temperature and 160 °C, which is attributed to the presence of water absorbed or bound to the fibers. Between 160 °C and 500 °C occurs the loss of mass attributed to the thermal degradation of organic compounds, such as cellulose, hemicellulose and lignin. Among these, the hemicellulose is the component of lower thermal stability, which is degraded between 180 °C and 260 °C. The cellulose degrades between 240 and 350 °C, and the lignin between 280 °C and 400 °C. At higher temperatures, degradation byproducts of cellulose, hemicellulose, and lignin are degraded [31]. For both fibers gravata and macauba, it was observed a higher intensity and a shift for higher temperatures of the 1st peak, after mercerizing and bleaching, which could be associated to the hemicellulose removal from the fibers and a consequent higher amount of cellulose on mercerized and bleached fibers [31].

Higher thermal stability can be observed for mercerized and bleached fibers, as well as narrowing and better definition of DTG peaks. This indicates that these treatments were efficient in the removal of compounds such as hemicellulose and lignin, as indicated by the XRD analyzes.

The characterization of vegetable fibers by FTIR is able to identify the presence of its main constituents: cellulose, hemicellulose and lignin. These components are composed mainly of alkanes and aromatic groups, as well as different functional groups containing oxygen, such as ester, ketone and alcohol [31,32], allowing monitoring the effect of chemical treatments on plant fibers.

Figure 5 shows the FTIR spectra of the raw, mercerized and bleached gravata and macauba fibers. Also indicated in the spectra are the absorption wave numbers of three characteristic bands: 1739  $\text{cm}^{-1}$ , relative to the stretching of C=O bonds of esters and carboxylic acids from hemicellulose; 1505  $\text{cm}^{-1}$  relative to the bonds of C=C of benzene rings present in the lignin, and 1247  $\text{cm}^{-1}$ , referring to the stretching of C=O bonds of acetyl groups belonging to lignin [31,32]. But it can be observed in the FTIR spectra that the three bands mentioned were totally or partially suppressed (except the band at 1505  $\text{cm}^{-1}$  for macauba), confirming the removal of hemicellulose and lignin from the gravata and macauba fibers.

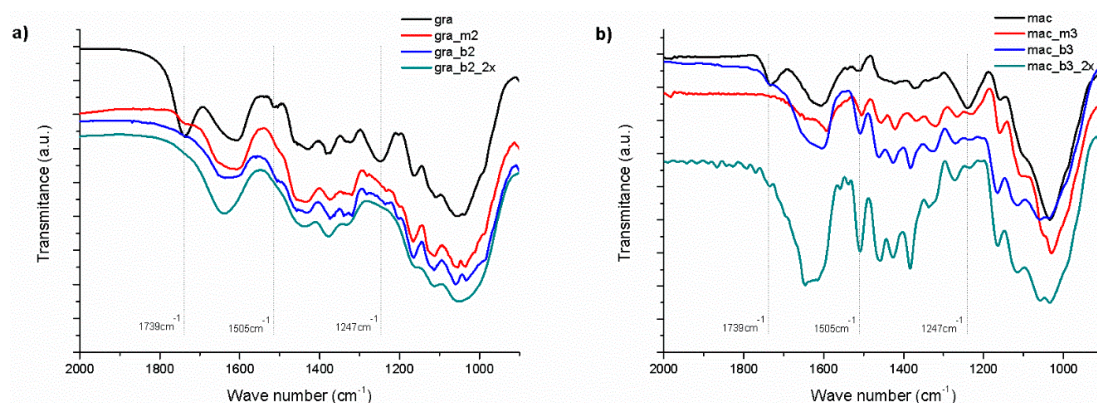


**Figure 5.** FTIR spectra of (a) gravata and (b) macauba: raw, mercerized and bleached fibers.

In order to observe the fiber surfaces before and after the treatments, SEM analyzes were carried out and Figure 6 present SEM images for raw, mercerized and bleached fibers of gravata and macauba.

The surfaces of the gravata and macauba fibers before the treatments are covered by impurities specific to the fibers, such as waxes and other types of fatty acids. It can also be observed that the mercerizing treatments were able to partially remove these impurities, exposing the cellulosic fibers. With the bleaching treatments, these cleaning and fibrillar exposure processes were maximized. From this higher cellulosic fibers exposure, it is expected to provide a greater efficiency of the acid hydrolysis step, increasing the yield in obtaining CNCs with a shorter reaction time.

Thus, it can be concluded that the most efficient treatments for the removal of non-cellulosic constituents were bleaching, performed once or twice. Thus, to continue the study of the production of cellulose nanocrystals from these fibers from Brazilian Pantanal, bleached fibers were used: gra\_b2, gra\_b2\_2x, mac\_b3 and mac\_b3\_2x.

In this way, CNC obtained from bleached fibers gra\_b2 and gra\_b2\_2x will be called CNCg\_1 and CNCg\_2, respectively. And the CNC obtained from mac\_b3 and mac\_b3\_2x will be called CNCm\_1 and CNCm\_2, respectively. And the termination corresponds to the hydrolysis time.

Figure 7 shows the cellulose nanocrystals from gravata (CNCg) and from macauba (CNCm), obtained via acid hydrolysis at different times of hydrolysis and after freeze-drying.

The obtained CNCs showed coloration in lighter and darker shades of brown. Higher hydrolysis time resulted on darker CNCg unlike CNCm, which remained with almost the same shade of brown. This darkening of CNCg may be related to some level of cellulose degradation caused by acid hydrolysis, since gravata cellulose fibrils were physically more exposed than those of macauba, as it can be observed by SEM images of pre-treated fibers. In addition, due to the higher exposure of the fibrils, there may have been a higher sulphonation of the CNCg with a longer hydrolysis time [33].

The morphology of the obtained CNCs was investigated by TEM analysis, and the micrographs of the CNCg and CNCm samples are presented in Figures 8 and 9, respectively.

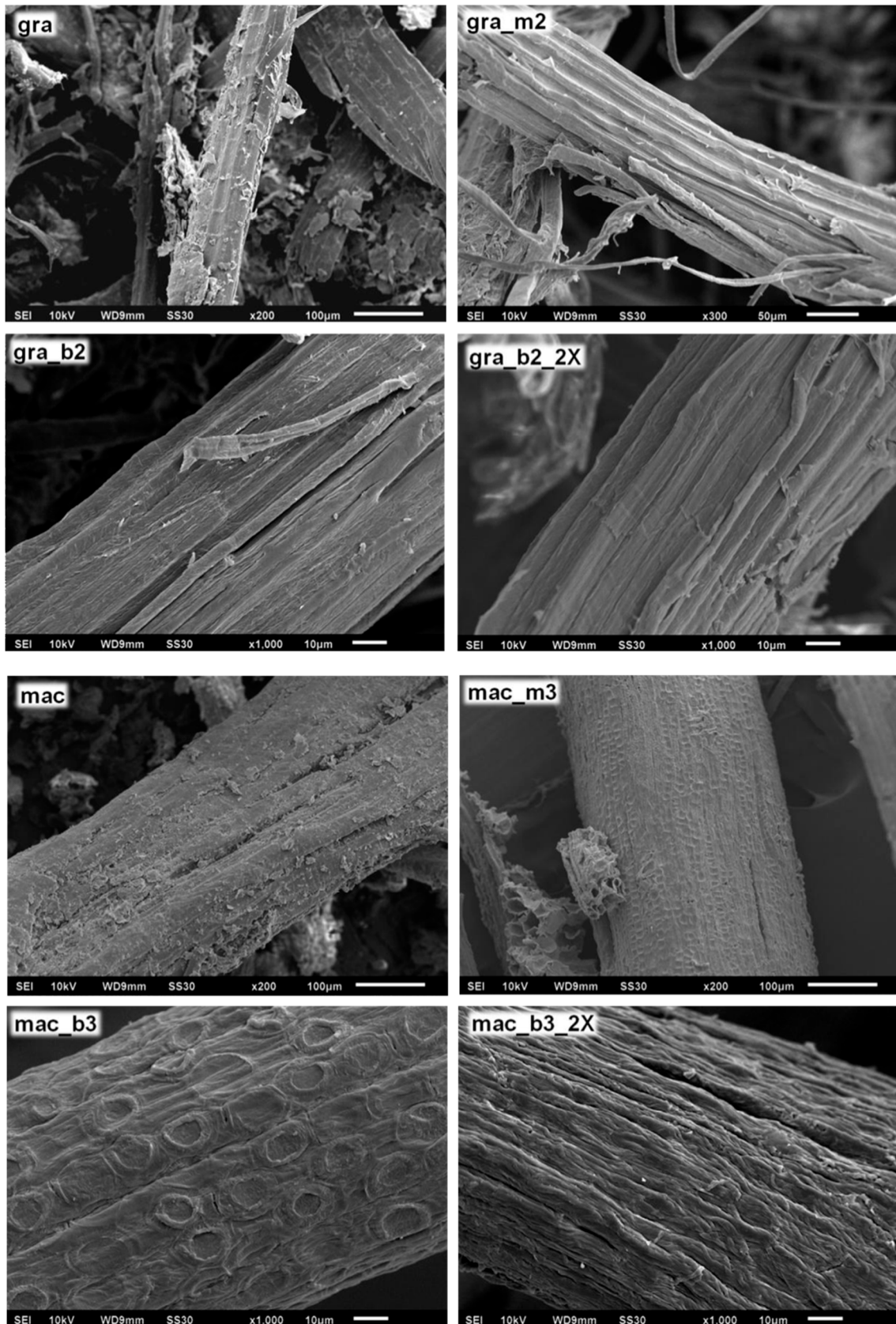


**Figure 6.** SEM micrographs of the surfaces of raw, mercerized and bleached fibers of gravata (gra) and macauba (mac).

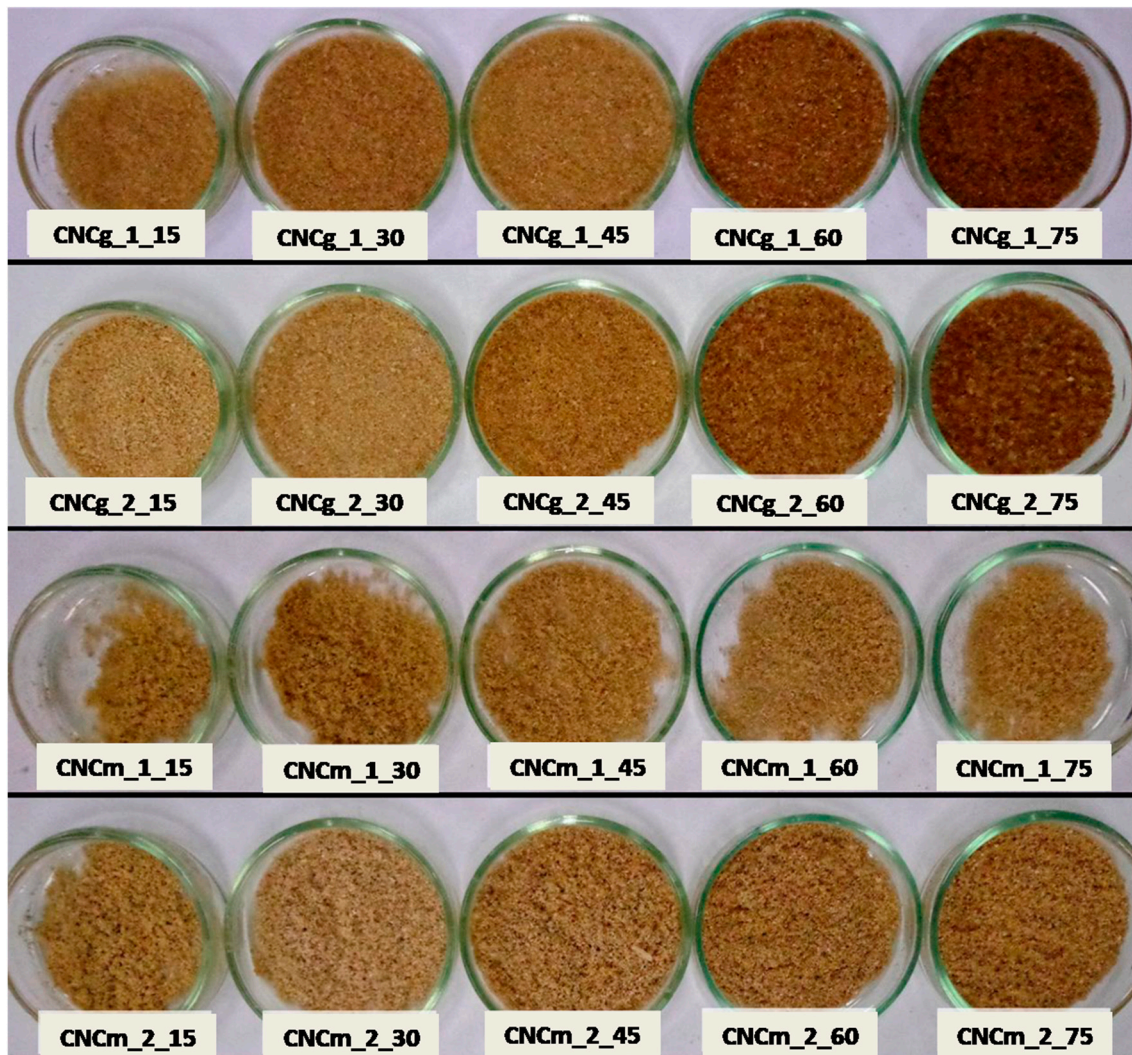


**Figure 7.** Visual aspect of CNCs from gravata and macauba fibers, after different times of acid hydrolysis and freeze-drying, with their respective encodings.

From the TEM images it was possible to observe individual CNCs, revealing their acicular forms at the nanoscale, very similar to CNCs obtained from other plant sources such as cotton, ramie, wheat, curauá, sisal, among others [14,16].

Lengths and diameters of the CNC were determined from TEM images, as well as their aspect ratio (L/D), which are presented in Table 4.

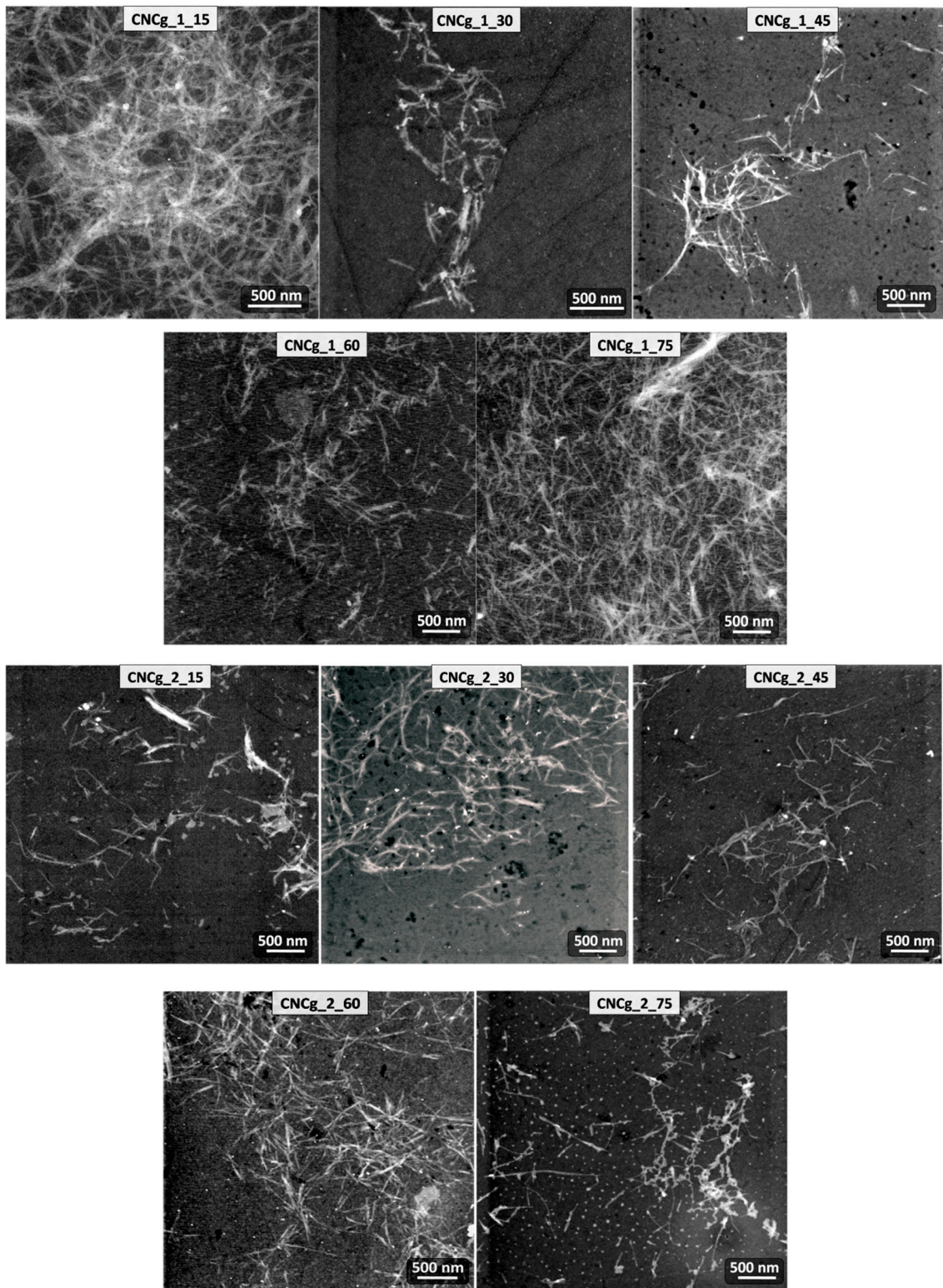


Figure 8. TEM micrographs of the CNCg samples with their respective encodings.

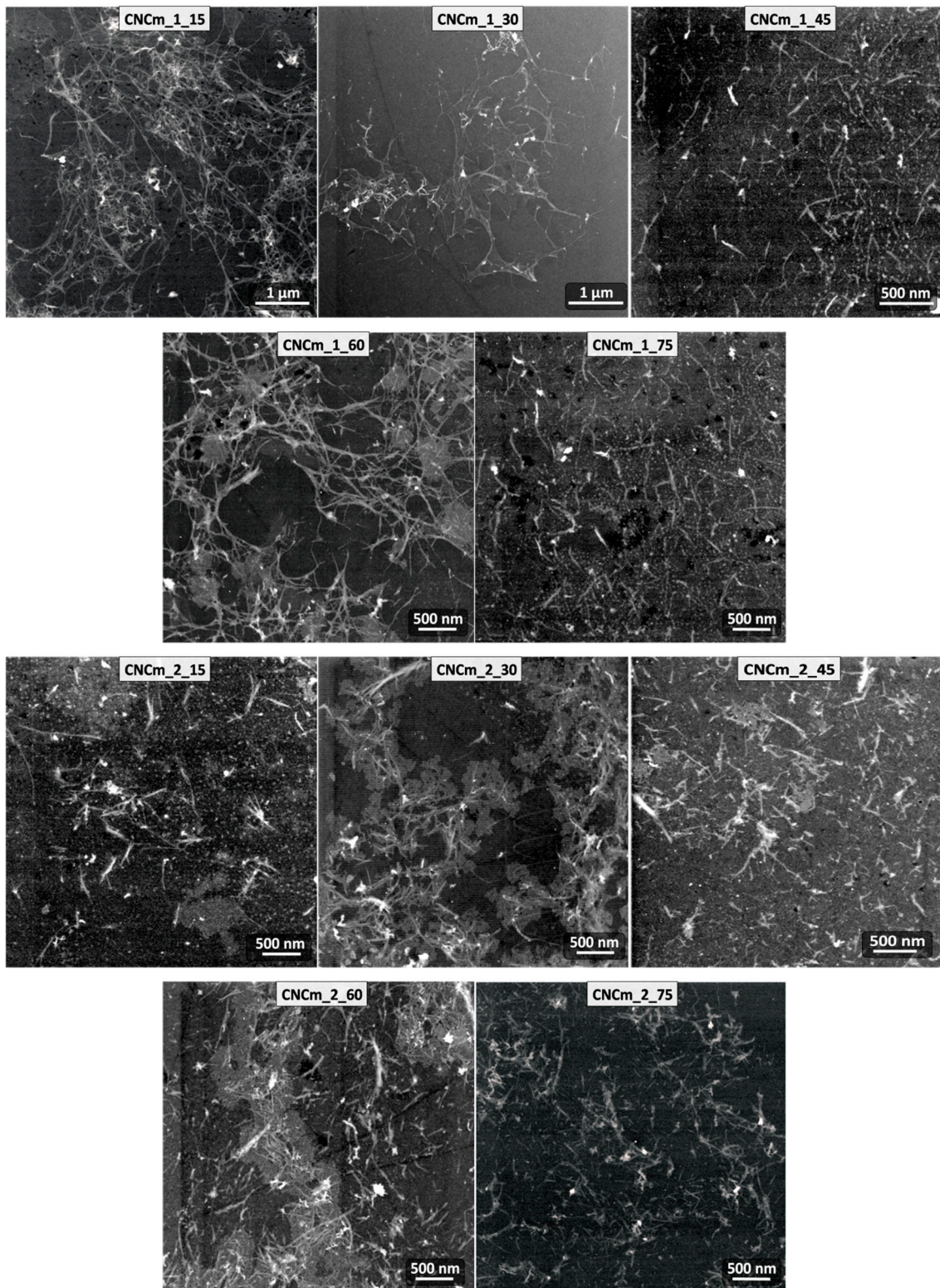


Figure 9. TEM micrographs of the CNCm samples with their respective encodings.

**Table 4.** Values of  $C_i$ ,  $T_{\text{onset}}$  and dimensions of CNC.

Sample	$C_i$ (%)	$T_{\text{onset}}$ (°C)	Length * (nm)	Diameter * (nm)	L/D
CNCg_1_15	80	268.6	582 ± 143 <sup>a</sup>	69 ± 22 <sup>a</sup>	8 ± 3
CNCg_1_30	80	259.2	322 ± 93 <sup>b</sup>	30 ± 8 <sup>b</sup>	10 ± 4
CNCg_1_45	82	264.2	345 ± 102 <sup>b</sup>	32 ± 10 <sup>b</sup>	11 ± 4
CNCg_1_60	76	250.3	289 ± 60 <sup>b,c</sup>	22 ± 4 <sup>c</sup>	13 ± 3
CNCg_1_75	73	235.1	257 ± 72 <sup>c,d</sup>	19 ± 8 <sup>c</sup>	14 ± 7
CNCg_2_15	87	276.5	373 ± 86 <sup>b,e</sup>	36 ± 8 <sup>b</sup>	10 ± 3
CNCg_2_30	87	258.5	386 ± 90 <sup>b,e</sup>	29 ± 7 <sup>b</sup>	13 ± 4
CNCg_2_45	88	263.5	383 ± 91 <sup>b,e</sup>	20 ± 4 <sup>c</sup>	19 ± 6
CNCg_2_60	84	249.0	282 ± 70 <sup>b,c,d</sup>	19 ± 4 <sup>c</sup>	15 ± 5
CNCg_2_75	82	240.6	217 ± 84 <sup>c,d</sup>	24 ± 8 <sup>c</sup>	9 ± 5
CNCm_1_15	78	230.5	499 ± 100 <sup>a</sup>	36 ± 7 <sup>a</sup>	14 ± 4
CNCm_1_30	79	230.2	462 ± 126 <sup>a</sup>	34 ± 12 <sup>a</sup>	13 ± 6
CNCm_1_45	81	231.0	428 ± 83 <sup>a,b</sup>	34 ± 8 <sup>a</sup>	13 ± 4
CNCm_1_60	83	227.8	359 ± 94 <sup>c</sup>	30 ± 8 <sup>a</sup>	12 ± 5
CNCm_1_75	80	224.6	231 ± 70 <sup>d</sup>	22 ± 4 <sup>b</sup>	10 ± 4
CNCm_2_15	83	234.7	410 ± 99 <sup>a,b,c</sup>	40 ± 12 <sup>c</sup>	10 ± 4
CNCm_2_30	83	237.7	377 ± 87 <sup>a,b,c</sup>	34 ± 7 <sup>a</sup>	11 ± 4
CNCm_2_45	86	237.7	304 ± 82 <sup>e</sup>	27 ± 8 <sup>a</sup>	11 ± 4
CNCm_2_60	80	230.6	238 ± 50 <sup>d</sup>	22 ± 5 <sup>b</sup>	11 ± 3
CNCm_2_75	77	194.8	171 ± 41 <sup>f</sup>	15 ± 4 <sup>c</sup>	11 ± 4

\* Values are averages of 50 measurements. Means accompanied by the same letter in the same column do not differ statistically according to the Tukey test.

From the average values of CNC lengths and diameters, it can be observed that there is a relationship between the CNC dimensions and the hydrolysis time. As the hydrolysis time increases, the length and diameter of the CNC are reduced [27]. It can also be observed that the number of bleaches that the fiber underwent prior to the step of hydrolysis interferes in the CNC dimensions only when these were obtained in shorter hydrolysis times (15 min, for example). Even at longer hydrolysis time, the number of bleaches in the fiber does not significantly change the average lengths and diameters of the CNC, as is the case, for example, of CNCg\_1\_75 and CNCg\_2\_75.

From the measurements of length and diameter of the CNC, it was possible to calculate their aspect ratios (L/D), an important parameter in relation to the use of them as reinforcement for polymer matrices, for example [34,35]. The L/D calculated values were in the range of 8 to 19, and the CNCg\_2\_45 presented the highest value. These values are in the range of values determined for other plant sources, such as sisal, curaua and cotton [12,14,16].

Regarding the crystalline structures of the obtained CNC, XRD analyzes were performed and Figure 10 present the XRD patterns for CNCg and CNCm, respectively.

The XRD profiles of CNCg and CNCm are similar to each other, showing characteristic peaks of cellulose type I with diffraction peaks at  $2\theta = 15^\circ$ ,  $17^\circ$  and  $22.7^\circ$  [2]. In addition, CNC showed the same characteristic peaks as their source fibers, demonstrating that the performed acid hydrolysis was not able to modify the cellulose crystal structure of the original fiber. On the other hand, the hydrolysis with strong acid has the capacity to remove non-cellulosic components of the vegetal fibers and also part of the amorphous fraction of cellulose, remaining the highly crystalline CNC.

The crystallinity indices of the CNC were determined by peak deconvolution of their XRD patterns and the determined values are given in Table 4. After acid hydrolysis there was an increase in  $C_i$  compared to those from bleached fibers. However, after longer hydrolysis times than 60 min the  $C_i$  values were reduced, indicating a possible destruction of the cellulose crystals. For both sources, gravata and macauba, the highest values of  $C_i$  were found around 45 min of acid hydrolysis.

The thermal behavior of the CNC was evaluated by thermogravimetry, and the TG/DTG curves of CNCg and CNCm are presented in Figure 11.

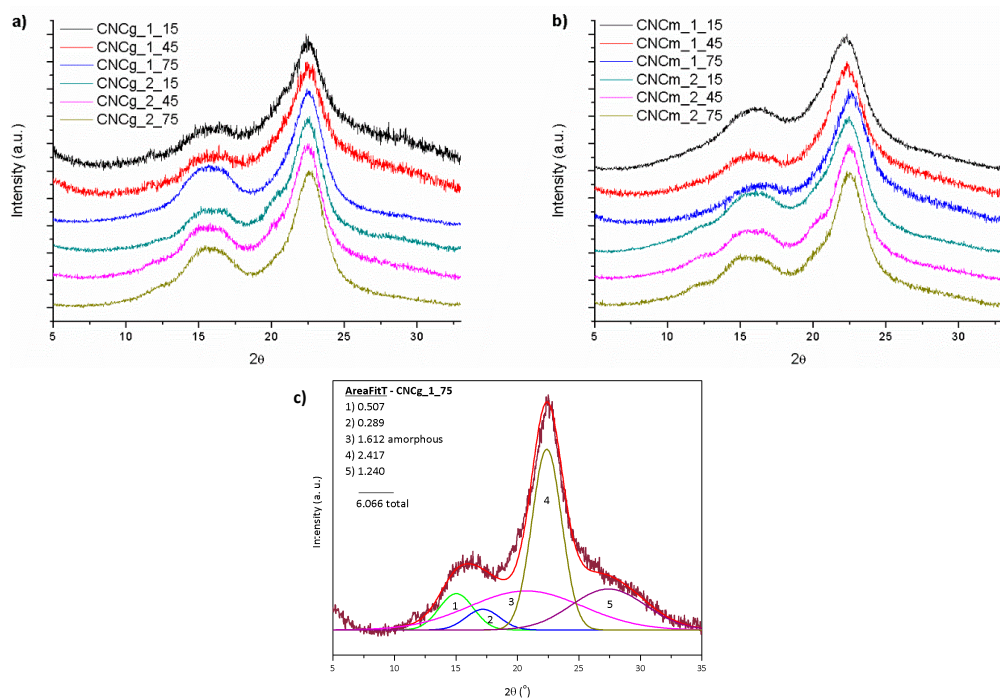


**Figure 10.** XRD profiles for the CNC obtained from (a) 1× and 2× bleached gravata fiber, (b) 1× and 2× bleached macauba fiber and (c) an example of deconvoluted peaks of CNCg\_1\_75.

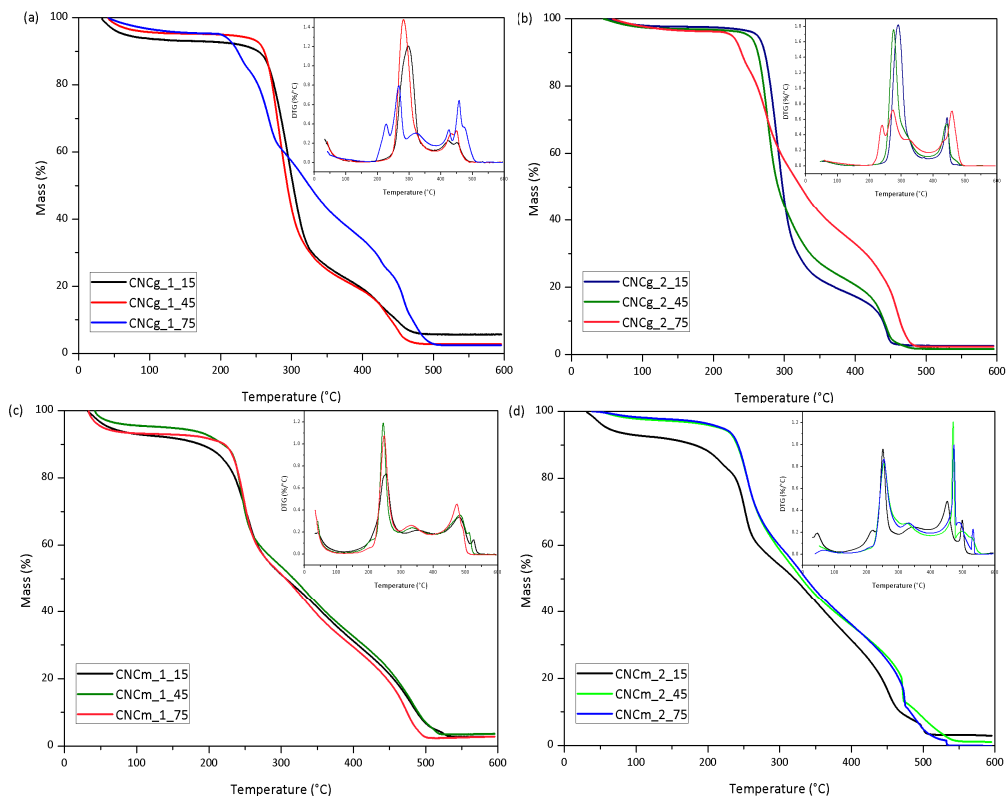


**Figure 11.** TG and DTG curves of CNCg obtained from (a) 1× and (b) 2× bleached gravata fiber; and CNCm obtained from (c) 1× and (d) 2× bleached macauba fiber; in synthetic air atmosphere and a heating rate of 10 °C/min.



The CNCs showed an initial mass loss up to approximately 120 °C, associated with water evaporation. Then, a stable plateau is made up to approximately 200 °C, where the thermooxidative degradation of the cellulose is initiated. The thermal degradation of the CNC starts at temperatures 50 °C to 80 °C lower than their respective bleached fibers. This phenomenon is associated with the incorporation of sulfate groups in the structure of cellulose, which exert a catalytic effect on the thermal degradation reaction of cellulose [36]. In this way, CNC obtained by the acid hydrolysis using sulfuric acid degrade at temperatures lower than its original vegetable fibers. Thus, the longer the acid hydrolysis using sulfuric acid, the higher the level of cellulose sulfation, and the lower the thermal stability of the CNC [16]. The reduction on thermal stability of CNC compared to those of treated fibers, caused by the incorporation of sulphate groups on cellulose surface, was also expressed on DTG peaks as a low density left shoulder (around 220 °C), particularly on CNCg\_1\_75 and CNCg\_2\_75.

The  $T_{\text{onset}}$  of the CNC were determined and are presented in Table 4. The CNCg presented higher thermal stabilities than the CNCm, comparing the same hydrolysis time and the same number of bleaching. The CNCg  $T_{\text{onset}}$  were in the range of 235 °C and 276 °C, whereas for the CNCm they varied between 195 °C and 237 °C. The superior thermally stable behavior of gravata in comparison to macauba was observed for the CNC as well, as it occurred with its raw and pretreated fibers. Thus, CNCg\_2\_45 presented the highest L/D and thermal stability, being suitable for incorporation into polymer matrices.

#### 4. Conclusions

Cellulose nanocrystals were extracted from macauba and gravata fibers successfully for the first time. TEM analyzes confirmed the obtaining of structures with nanometric dimensions and with acicular formats. The increase in hydrolysis time resulted in both the decrease in lengths (between 580 and 190 nm) and diameters (between 69 and 15 nm) of CNCg and CNCm.

The crystallinity indices of the CNCs began to present reductions after 45 min of hydrolysis, indicating that longer times of acid hydrolysis degrade the cellulosic crystals of CNCg and CNCm.

The thermal stabilities of CNC were between 195 °C and 260 °C, but longer hydrolysis time reduced CNC thermal stability. CNCg were more thermally stable than CNCm. These thermal stabilities indicated the potential of application of these CNC in polymer matrices, such as TPS/PCL, for the development of biodegradable nanocomposites.

Aiming the development of new bionanocomposites, CNC from gravatá, specifically CNCg\_2\_45, showed higher thermal stability and L/D, which are important parameters to provide wider processing windows and improved mechanical properties to bionanocomposites.

**Author Contributions:** Conceptualization, A.C.C. and V.B.C.; Formal analysis, A.C.C.; Supervision, F.G., J.M.M. and L.H.C.M.; Writing – original draft, V.B.C.; Writing – review & editing, A.C.C. and J.A.S.

**Acknowledgments:** This study was financed in part by the Coordenação de Aperfeiçoamento de Pessoal de Nível Superior - Brasil (CAPES) - Finance Code 001(1069810) and 88887.362968/2019-00. The authors would like to thank to financial support given by CNPq, SISNANO/MCTI, FINEP and Embrapa AgroNano research network. The authors also thank the Laboratory of Structural Characterization (LCE/DEMa/UFSCar) for the general facilities.

**Conflicts of Interest:** The authors declare no conflict of interest.

#### References

1. Dufresne, A. Cellulose nanomaterials as green nanoreinforcements for polymer nanocomposites. *Philos. Trans. R. Soc. A Math. Phys. Eng. Sci.* **2018**, *376*, 20170040. [[CrossRef](#)] [[PubMed](#)]
2. Klemm, D.; Heublein, B.; Fink, H.P.; Bohn, A. Cellulose: Fascinating Biopolymer and Sustainable Raw Material. *Angew. Chem. Int. Ed.* **2005**, *44*, 3358–3393. [[CrossRef](#)] [[PubMed](#)]
3. Klemm, D.; Kramer, F.; Moritz, S.; Lindström, T.; Ankerfors, M.; Gray, D.; Dorris, A. Nanocelluloses: A New Family of Nature-Based Materials. *Angew. Chem. Int. Ed.* **2011**, *50*, 5438–5466. [[CrossRef](#)]
4. Bondeson, D.; Mathew, A.; Oksman, K. Optimization of the isolation of nanocrystals from microcrystalline cellulose by acid hydrolysis. *Cellulose* **2006**, *13*, 171–180. [[CrossRef](#)]

5. Beck-Candanedo, S.; Roman, M.; Gray, D.G. Effect of Reaction Conditions on the Properties and Behavior of Wood Cellulose Nanocrystal Suspensions. *Biomacromolecules* **2005**, *6*, 1048–1054. [[CrossRef](#)]
6. Silva, R.; Haraguchi, S.K.; Muniz, E.C.; Rubira, A.F. Aplicações de fibras lignocelulósicas na química de polímeros e em compósitos. *Química Nova* **2009**, *32*, 661–671. [[CrossRef](#)]
7. Eichhorn, S.J. Cellulose nanowhiskers: Promising materials for advanced applications. *Soft Matter* **2011**, *7*, 303–315. [[CrossRef](#)]
8. Favier, V.; Chanzy, H.; Cavaille, J.Y. Polymer Nanocomposites Reinforced by Cellulose Whiskers. *Macromolecules* **1995**, *28*, 6365–6367. [[CrossRef](#)]
9. Araki, J.; Kuga, S. Effect of Trace Electrolyte on Liquid Crystal Type of Cellulose Microcrystals. *Langmuir* **2001**, *17*, 4493–4496. [[CrossRef](#)]
10. Tonoli, G.H.D.; Teixeira, E.M.; Corrêa, A.C.; Marconcini, J.M.; Caixeta, L.A.; Pereira-da-Silva, M.A.; Mattoso, L.H.C. Cellulose micro/nanofibres from Eucalyptus kraft pulp: Preparation and properties. *Carbohydr. Polym.* **2012**, *89*, 80–88. [[CrossRef](#)]
11. Martins, M.A.; Teixeira, E.M.; Corrêa, A.C.; Ferreira, M.; Mattoso, L.H. Extraction and characterization of cellulose whiskers from commercial cotton fibers. *J. Mater. Sci.* **2011**, *46*, 7858–7864. [[CrossRef](#)]
12. de Morais Teixeira, E.; Corrêa, A.C.; Manzoli, A.; de Lima Leite, F.; de Oliveira, C.R.; Mattoso, L.H.C. Cellulose nanofibers from white and naturally colored cotton fibers. *Cellulose* **2010**, *17*, 595–606. [[CrossRef](#)]
13. de Morais Teixeira, E.; Bondancia, T.J.; Teodoro, K.B.R.; Corrêa, A.C.; Marconcini, J.M.; Mattoso, L.H.C. Sugarcane bagasse whiskers: Extraction and characterizations. *Ind. Crop. Prod.* **2011**, *33*, 63–66. [[CrossRef](#)]
14. Teodoro, K.B.; Teixeira, E.D.M.; Corrêa, A.C.; Campos, A.D.; Marconcini, J.M.; Mattoso, L.H. Whiskers de fibra de sisal obtidos sob diferentes condições de hidrólise ácida: Efeito do tempo e da temperatura de extração. *Polímeros* **2011**, *21*, 280–285. [[CrossRef](#)]
15. Campos, A.; Teodoro, K.B.R.; Teixeira, E.M.; Corrêa, A.C.; Marconcini, J.M.; Wood, D.F.; Williams, T.G.; Mattoso, L.H.C. Properties of thermoplastic starch and TPS/polycaprolactone blend reinforced with sisal whiskers using extrusion processing. *Polym. Eng. Sci.* **2013**, *53*, 800–808. [[CrossRef](#)]
16. Corrêa, A.C.; de Morais Teixeira, E.; Pessan, L.A.; Mattoso, L.H.C. Cellulose nanofibers from curauá fibers. *Cellulose* **2010**, *17*, 1183–1192. [[CrossRef](#)]
17. Araki, J.; Wada, M.; Kuga, S.; Okano, T. Flow properties of microcrystalline cellulose suspension prepared by acid treatment of native cellulose. *Colloids Surf. A Physicochem. Eng. Asp.* **1998**, *142*, 75–82. [[CrossRef](#)]
18. Revol, J.F.; Godbout, L.; Dong, X.M.; Gray, D.G.; Chanzy, H.; Maret, G. Chiral nematic suspensions of cellulose crystallites; phase separation and magnetic field orientation. *Liq. Cryst.* **1994**, *16*, 127–134. [[CrossRef](#)]
19. Terech, P.; Chazeau, L.; Cavaille, J.Y. A Small-Angle Scattering Study of Cellulose Whiskers in Aqueous Suspensions. *Macromolecules* **1999**, *32*, 1872–1875. [[CrossRef](#)]
20. Hanley, S.J.; Revol, J.F.; Godbout, L.; Gray, D.G. Atomic force microscopy and transmission electron microscopy of cellulose from *Micrasterias denticulata*; evidence for a chiral helical microfibril twist. *Cellulose* **1997**, *4*, 209–220. [[CrossRef](#)]
21. Teixeira, E.D.M.; de Oliveira, C.R.; Mattoso, L.H.; Corrêa, A.C.; Paladin, P.D. Nanofibras de algodão obtidas sob diferentes condições de hidrólise ácida. *Polímeros* **2010**, *20*, 264–268. [[CrossRef](#)]
22. Kumar, A.P.; Singh, R.P. Biocomposites of cellulose reinforced starch: Improvement of properties by photo-induced crosslinking. *Bioresour. Technol.* **2008**, *99*, 8803–8809. [[CrossRef](#)] [[PubMed](#)]
23. Teixeira, E.D.M.; Pasquini, D.; Curvelo, A.A.; Corradini, E.; Belgacem, M.N.; Dufresne, A. Cassava bagasse cellulose nanofibrils reinforced thermoplastic cassava starch. *Carbohydr. Polym.* **2009**, *78*, 422–431. [[CrossRef](#)]
24. Carmona, V.B. Desenvolvimento de blendas de TPS, PCL E PLA e seus nanocompósitos com nanowhiskers de celulose de gravatá. Ph.D. Thesis, Federal University of São Carlos, São Carlos, Brazil, 2015.
25. Simão, J.A. Avaliação de fibras de gravatá, macaúba e curauá para aplicação em compósitos de polipropileno obtidos por mistura termocinética. Ph.D. Thesis, Federal University of Sao Carlos, São Carlos, Brazil, 2018.
26. Pott, A.; Pott, V.J. *Plantas do Pantanal*; EMBRAPA Comunicação para transferência de Tecnologia: Brasília, Brazil, 1994.
27. Campos, A.D.; Neto, A.R.; Rodrigues, V.B.; Kuana, V.A.; Correa, A.C.; Takahashi, M.C.; Mattoso, L.H.; Marconcini, J.M. Production of Cellulose Nanowhiskers from Oil Palm Mesocarp Fibers by Acid Hydrolysis and Microfluidization. *J. Nanosci. Nanotechnol.* **2017**, *17*, 4970–4976. [[CrossRef](#)]

28. Oh, S.Y.; Yoo, D.I.; Shin, Y.; Kim, H.C.; Kim, H.Y.; Chung, Y.S.; Park, W.H.; Youk, J.H. Crystalline structure analysis of cellulose treated with sodium hydroxide and carbon dioxide by means of X-ray diffraction and FTIR spectroscopy. *Carbohydr. Res.* **2005**, *340*, 2376–2391. [[CrossRef](#)]
29. Thygesen, A.; Oddershede, J.; Lilholt, H.; Thomsen, A.B.; Ståhl, K. On the determination of crystallinity and cellulose content in plant fibres. *Cellulose* **2005**, *12*, 563–576. [[CrossRef](#)]
30. Borysiak, S.; Garbarczyk, J. Applying the WAXS method to estimate the supermolecular structure of cellulose fibres after mercerisation. *Fibres Text. East. Eur.* **2003**, *11*, 104–106.
31. Tomczak, F.; Sydenstricker, T.H.D.; Satyanarayana, K.G. Studies on lignocellulosic fibers of Brazil. Part II: Morphology and properties of Brazilian coconut fibers. *Compos. Part A Appl. Sci. Manuf.* **2007**, *38*, 1710–1721. [[CrossRef](#)]
32. Liu, W.; Mohanty, A.K.; Drzal, L.T.; Askel, P.; Misra, M. Effects of alkali treatment on the structure, morphology and thermal properties of native grass fibers as reinforcements for polymer matrix composites. *J. Mater. Sci.* **2004**, *39*, 1051–1054. [[CrossRef](#)]
33. Jarvis, M.C. Structure of native cellulose microfibrils, the starting point for nanocellulose manufacture. *Philos. Trans. R. Soc. A Math. Phys. Eng. Sci.* **2018**, *376*, 20170045. [[CrossRef](#)]
34. Halpin, J.C.; Kardos, J.L. Moduli of Crystalline Polymers Employing Composite Theory. *J. Appl. Phys.* **1972**, *43*, 2235–2241. [[CrossRef](#)]
35. Ouali, N.; Cavaille, J.-Y.; Perez, J. Elastic Viscoelastic and Plastic Behavior of Multiphase polymer blends. *Plast. Rubber Compos. Process. Appl.* **1991**, *16*, 55–60.
36. Roman, M.; Winter, W.T. Effect of Sulfate Groups from Sulfuric Acid Hydrolysis on the Thermal Degradation Behavior of Bacterial Cellulose. *Biomacromolecules* **2004**, *5*, 1671–1677. [[CrossRef](#)] [[PubMed](#)]



© 2019 by the authors. Licensee MDPI, Basel, Switzerland. This article is an open access article distributed under the terms and conditions of the Creative Commons Attribution (CC BY) license (<http://creativecommons.org/licenses/by/4.0/>).